

Supplementary Materials for **Dependence of drivers affects risks associated with compound events**

Jakob Zscheischler and Sonia I. Seneviratne

Published 28 June 2017, *Sci. Adv.* **3**, e1700263 (2017)

DOI: 10.1126/sciadv.1700263

This PDF file includes:

- table S1. Global climate models used in this study, with number of runs in brackets.
- fig. S1. Fraction of CMIP5 models with negative correlation between temperature and precipitation.
- fig. S2. Effective return period of extremely hot and dry warm seasons.
- fig. S3. Difference in the number of concurrently extreme hot and dry warm seasons between 1870–1969 and 2001–2100.
- fig. S4. Change in likelihood that hot and dry warm seasons with return periods of 20 and 50 years during 1870–1969 will occur during the 21st century.
- fig. S5. Comparison of correlations of temperature and precipitation between CMIP5 and observation-based data sets.
- fig. S6. Difference in correlation of temperature and precipitation between original and detrended data.
- fig. S7. Serial correlation in seasonal temperature and precipitation averaged over the warm season.
- fig. S8. Random samples of the four Archimedean copulas used in this study.

table S1. Global climate models used in this study, with number of runs in brackets.

ACCESS1-0	CMCC-CM	GISS-E2-H	IPSL-CM5B-LR
ACCESS1-3	CMCC-CMS	GISS-E2-H-CC	MIROC-ESM
bcc-csm1-1	CNRM-CM5 (5)	GISS-E2-R	MIROC-ESM-CHEM
bcc-csm1-1-m	CSIRO-Mk3-6-0 (10)	GISS-E2-R-CC	MIROC5 (3)
BNU-ESM	EC-EARTH (6)	HadGEM2-AO	MPI-ESM-LR (3)
CanESM2 (5)	FGOALS-g2	HadGEM2-CC	MPI-ESM-MR
CCSM4 (6)	FIO-ESM (3)	HadGEM2-ES (4)	MRI-CGCM3
CESM1-BGC	GFDL-CM3	inmcm4	MRI-ESM1
CESM1-CAM5 (3)	GFDL-ESM2G	IPSL-CM5A-LR (4)	NorESM1-M
CMCC-CESM	GFDL-ESM2M	IPSL-CM5A-MR	NorESM1-ME

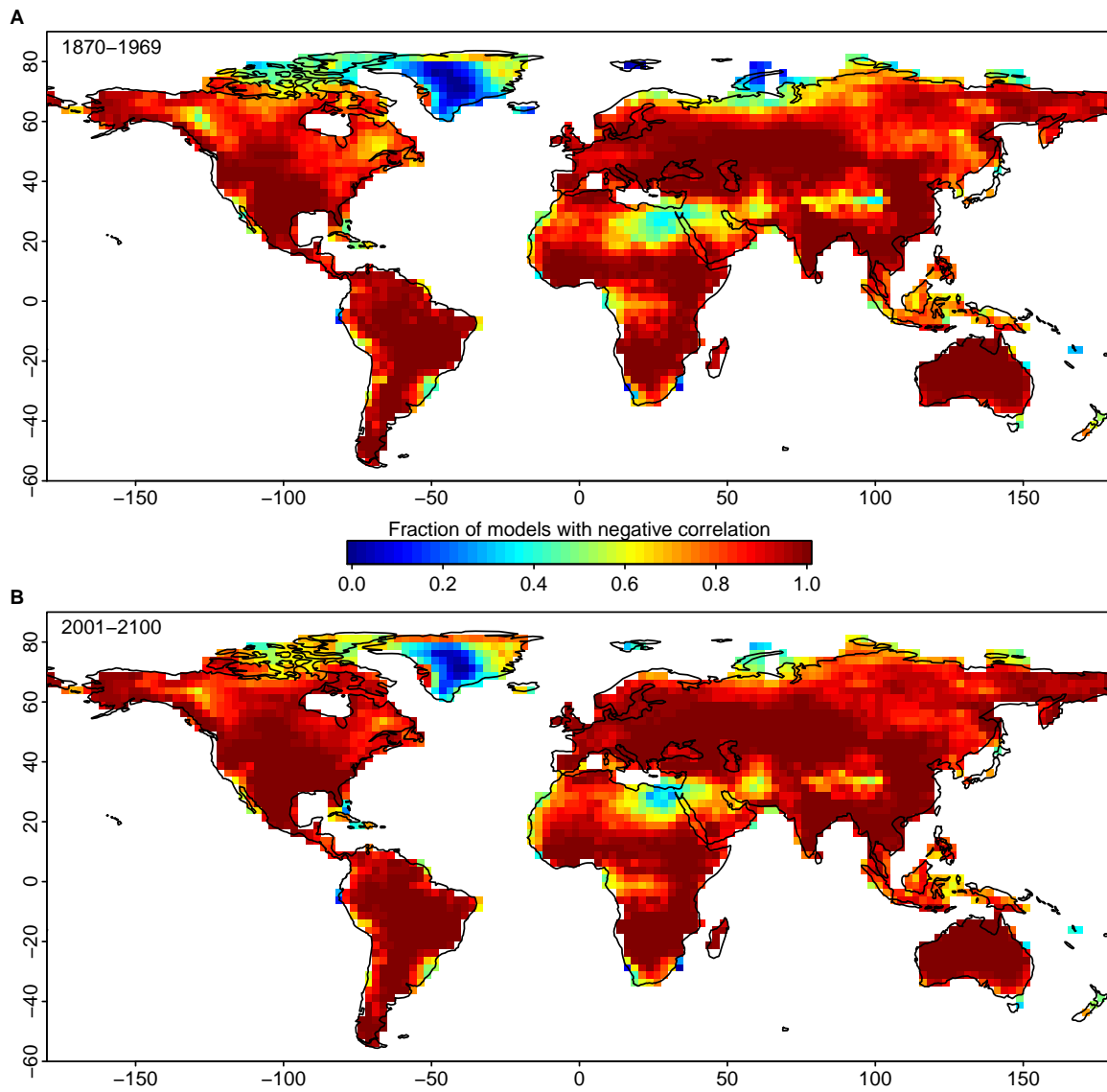


fig. S1. Fraction of CMIP5 models with negative correlation between temperature and precipitation. Fraction of models for which the correlation between detrended temperature and detrended precipitation averaged over the warm season is less or equal 0. (A) 1870-1969 (B) 2001-2100.

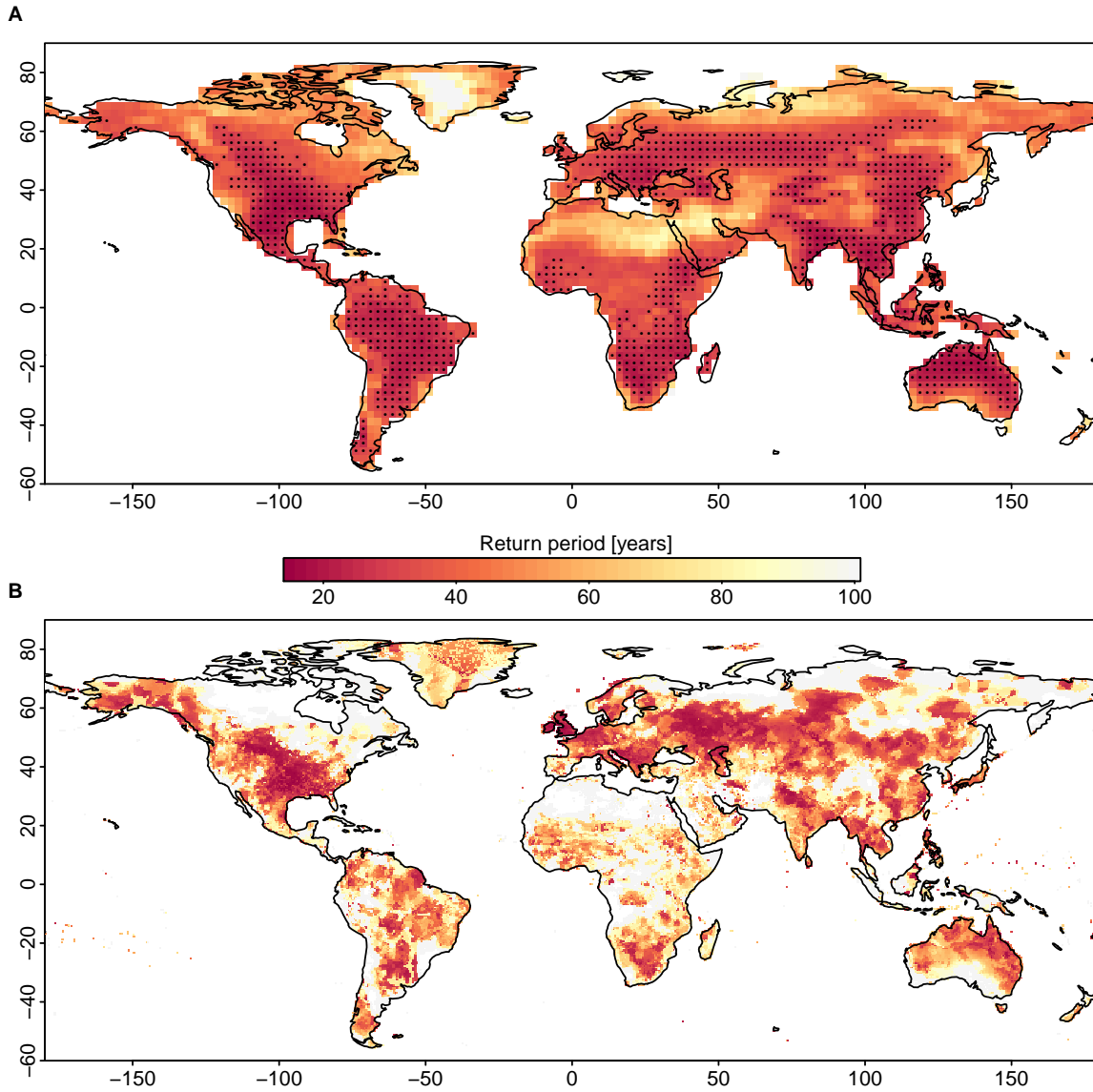


fig. S2. Effective return period of extremely hot and dry warm seasons. Return period of extremely hot and dry warm seasons, that is, temperature and negative precipitation averaged over the warm season concurrently exceed their 90th percentile. This return period would be 100 years if temperature and precipitation were independent but is much lower if negative correlation of temperature and precipitation is taken into account. **(A)** Average of all CMIP5 models. **(B)** Average of datasets CRU, Princeton, and Delaware.

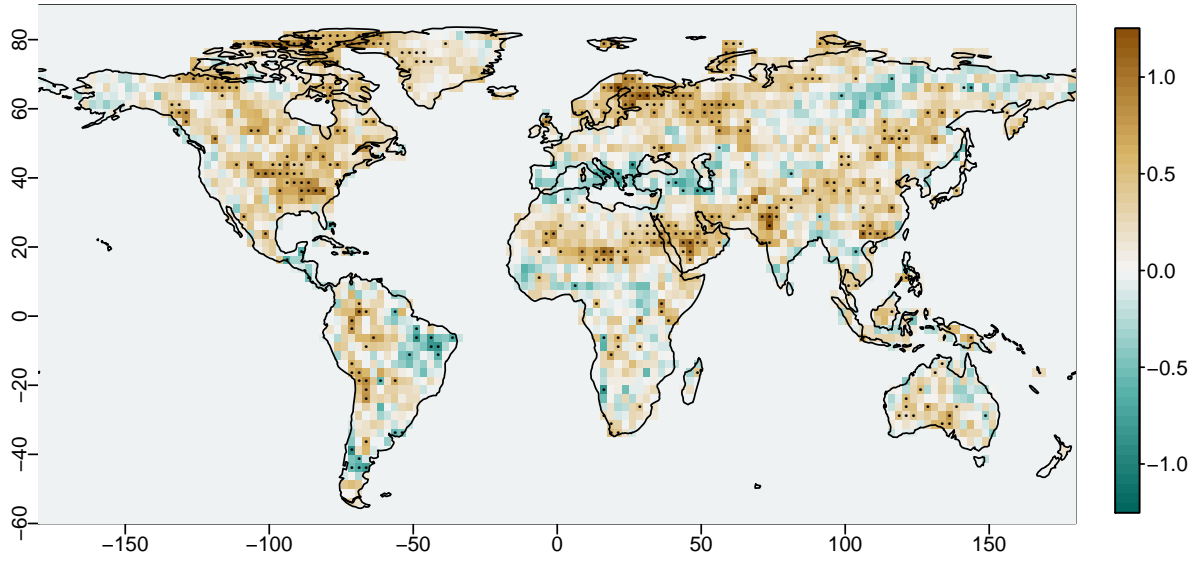


fig. S3. Difference in the number of concurrently extreme hot and dry warm seasons between 1870–1969 and 2001–2100. We first defined thresholds for temperature and negative precipitation as their 90th percentiles for the time period 1870-1969. We then computed the difference in number of years between 1870-1969 and 2001-2100 (based on RCP8.5) in which temperature and negative precipitation concurrently exceed these thresholds. Shown is the average over all CMIP5 models. Temperature and precipitation were detrended prior to computing the exceedances.

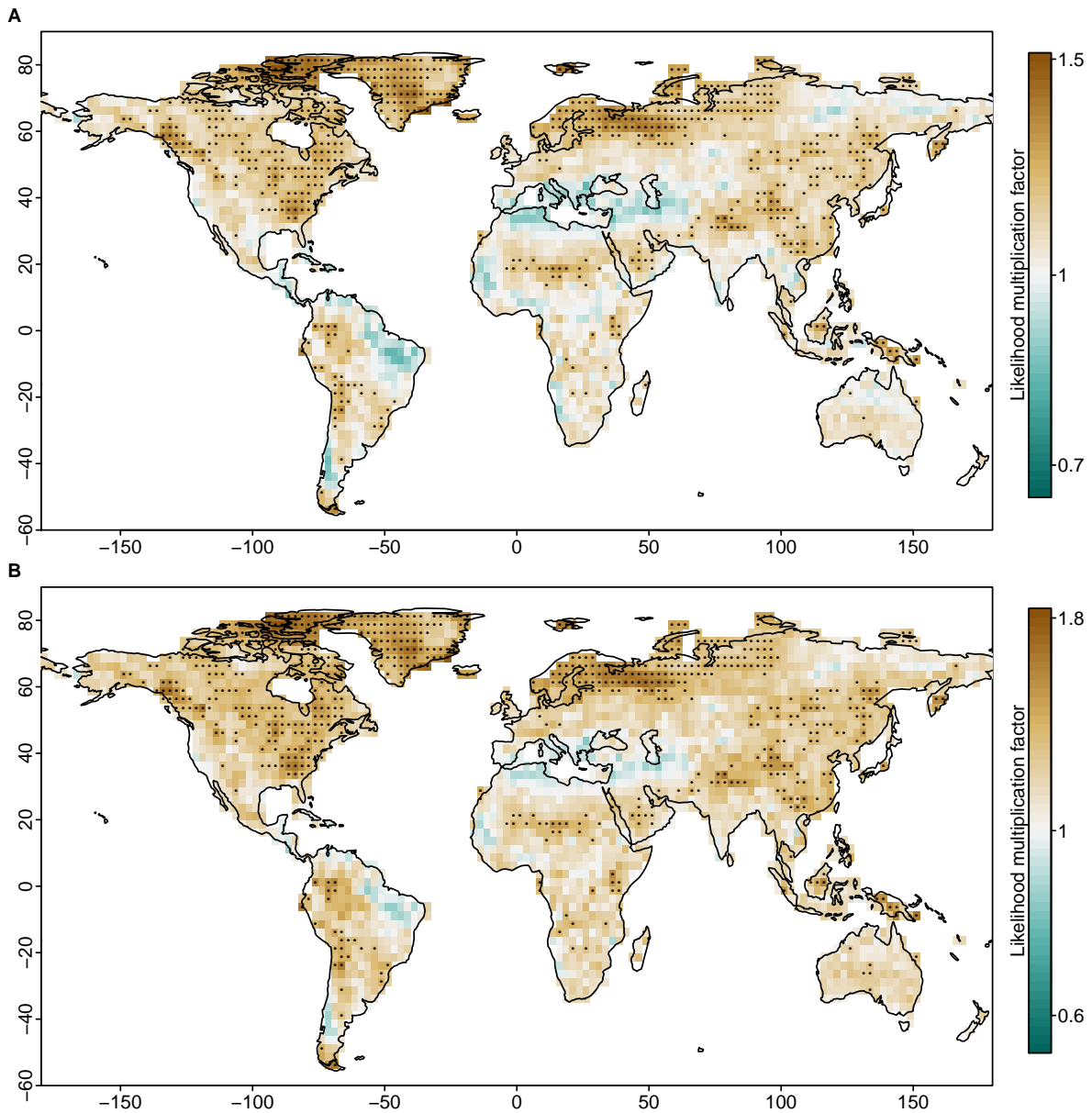


fig. S4. Change in likelihood that hot and dry warm seasons with return periods of 20 and 50 years during 1870–1969 will occur during the 21st century. In analogy to Figure 4C but for 20- (A) and 50-year events (B). Shown is the change in likelihood as a multiplicative factor, averaged across all CMIP5 models. Stippling highlights locations where models show a significant increase in likelihood in the 21st century (adjusted $P < 0.1$).

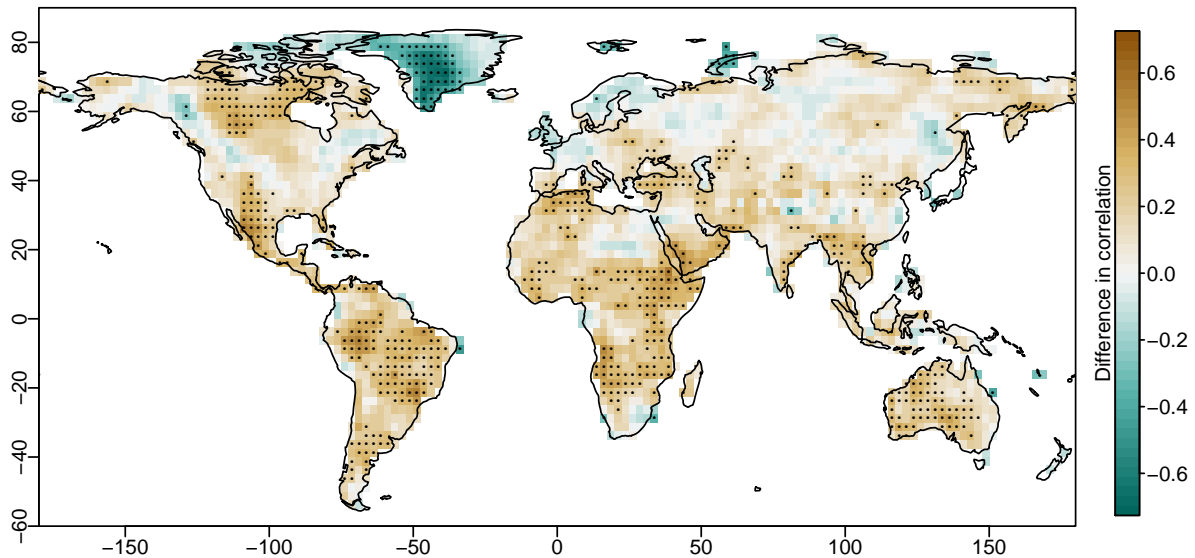


fig. S5. Comparison of correlations of temperature and precipitation between CMIP5 and observation-based data sets. Correlations were computed between temperature and precipitation averaged over the warm season for each model and observations-based dataset. Shown is the difference between the average of the correlations in CMIP5 models and the average of the correlations of observation-based datasets. Crosses denotes grid cells where observation-based datasets fall outside the 10th-to-90th percentile range of the CMIP5 models. This is the case for 25% the land area, denoting either large uncertainties in the observations-based datasets or a systematic bias in the CMIP5 models.

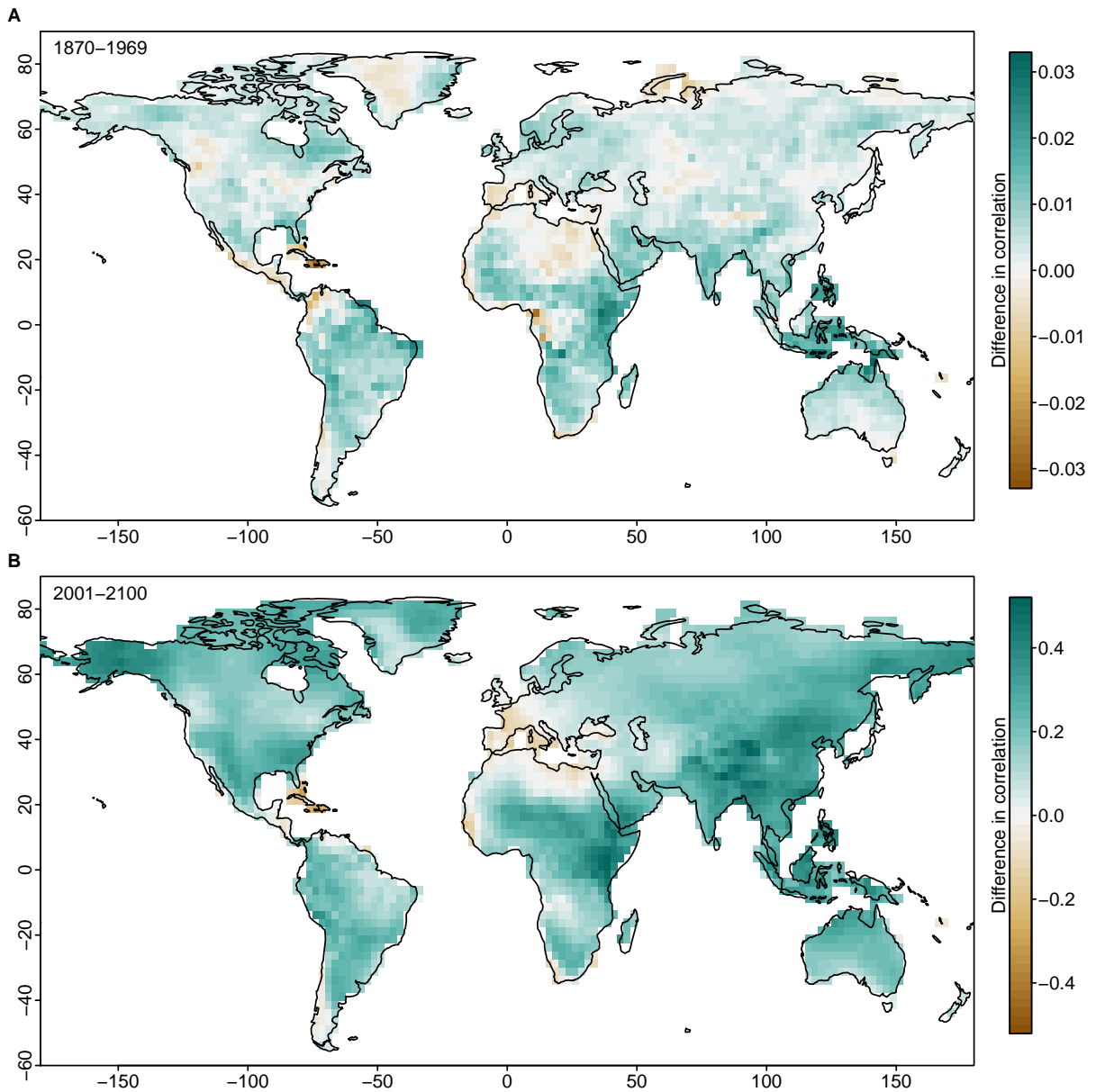


fig. S6. Difference in correlation of temperature and precipitation between original and detrended data. Difference in the interannual correlation between temperature and precipitation averaged over the warm season between original and linearly detrended data. Correlations were computed for each model and then averaged over all CMIP5 models. (A) 1870-1969. (B) 2001-2100.

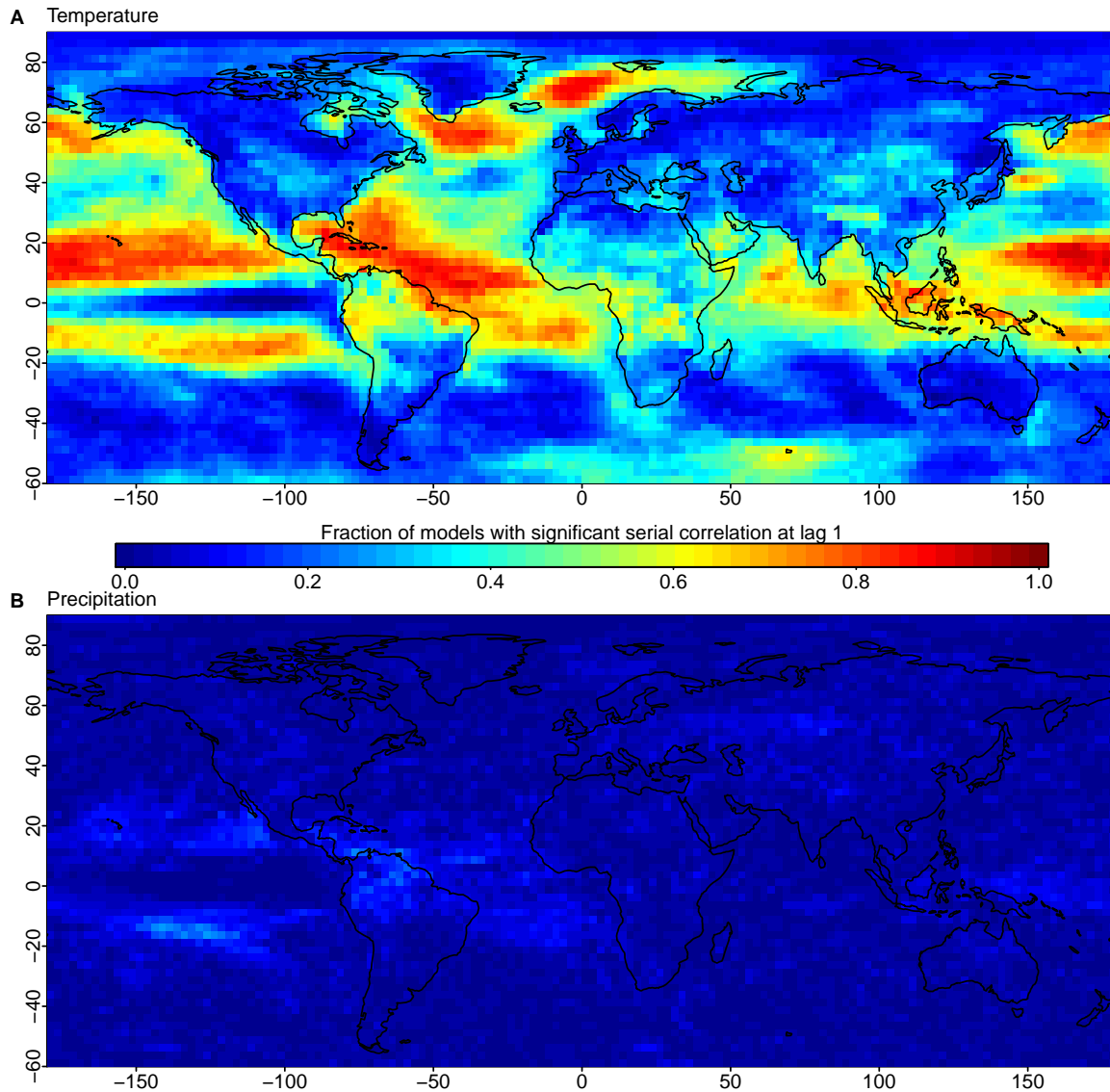


fig. S7. Serial correlation in seasonal temperature and precipitation averaged over the warm season. Fraction of CMIP5 models with significant serial correlation at lag 1 ($P < 0.05$) for temperature (**A**) and precipitation (**B**) averaged over the warm season during the time period 1870-1969.

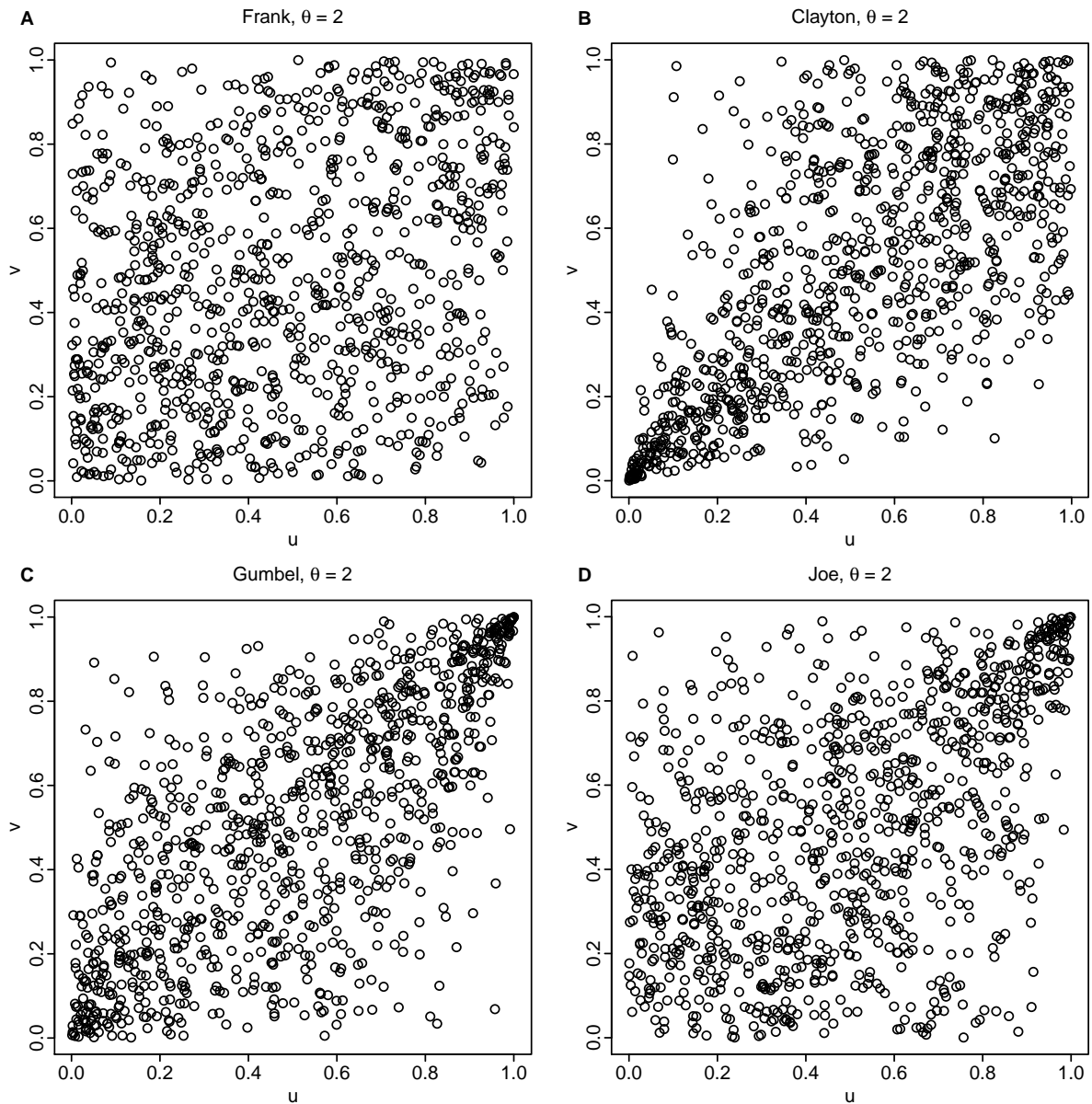


fig. S8. Random samples of the four Archimedean copulas used in this study. Shown are 1000 random samples from a Frank (A), Clayton (B), Gumbel (C), and Joe (D) copula, with $\theta = 2$ each time. For the Clayton copula, very small values are correlated, for the Gumbel and Joe copula, very large values are correlated. For the Frank copula, there is no dependence in the tails.